Available online at www.sciencedirect.com
ScienceDirect
Mechanics of Materials 39 (2007) 746–752
MECHANICS OF MATERIALS
www.elsevier.com/locate/mechmat

On size effect of cleavage cracking in polycrystalline thin films

Y. Qiao *, X. Kong

Department of Structural Engineering, University of California at San Diego, La Jolla, CA 92093-0085, USA

Received 14 September 2005

Abstract

A crack trapping model is developed for the fracture resistance of high-angle grain boundaries in free-standing brittle thin films, based on which a new size effect is predicted. In addition to the crystallographic misorientations, the grain boundary toughness is also dependent on the film thickness, primarily due to the geometrically necessary crack front branching.

Keywords: Size effect; Cleavage cracking; Free-standing; Thin film; Crack trapping

1. Introduction

With the progress in the development of thin film materials such as silicon, silica, alumina, and gallium arsenide and nitride that have been widely applied in microfabrication, the size effect associated with their mechanical behaviors has been an active research field for many years (e.g. Ohring, 2002). It is well known that the strength of a thin solid film is highly dependent on its thickness, for which a number of models, including strain gradient theories and geometrically necessary dislocation theories, have been established (Gao et al., 1999; Hutchinson and Evans, 2000). At working temperatures, many of thin film materials are brittle, for which cleavage cracking is the dominant fracture mechanism. However, currently, the studies on the size effect in failure processes are rare.

Fig. 1 depicts a cleavage crack in a free-standing polycrystalline thin film. In the deposition process the unfavorable grains would be buried and eventually most of the grains are through thickness (Madou, 2002). If the temperature is relatively low, the grains are columnar, otherwise the grain structure can be equiaxed. The cross-sectional diameters of grains are usually in the range of 0.1–10 μm. Depending on the processing parameters such as the back pressure and the deposition rate, the grain orientation of the film can be either random or textured. In either case, the grain boundaries interrupt the cracking processes in individual grains; that is, the fracture surface must transmit from the cleavage plane of one grain to that of the other as the crack propagates across a grain boundary (Gell and Smith, 1967).

* Corresponding author. Tel.: +1 858 534 3388; fax: +1 858 822 2260.
E-mail address: yqiao@ucsd.edu (Y. Qiao).

0167-6636/$ - see front matter © 2007 Elsevier Ltd. All rights reserved.
doi:10.1016/j.mechmat.2006.12.003

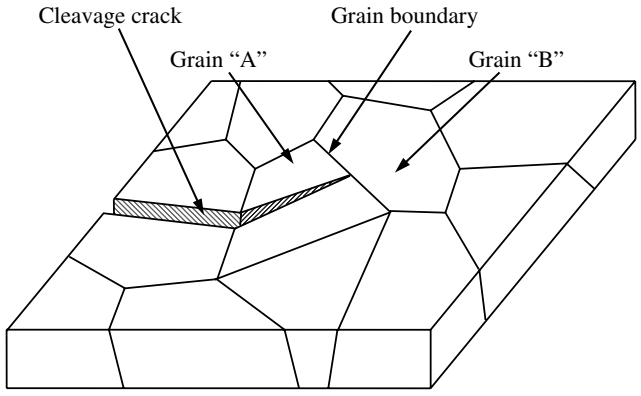

Fig. 1. A schematic diagram of a cleavage crack arrested by a grain boundary in a free-standing polycrystalline thin film.

In a previous experimental study (Qiao and Argon, 2003a,b), it was observed that, when a cleavage front reaches a grain boundary, it would first penetrate stably across the boundary at a number of break-through points. The distance between the break-through points ranges from 0.1 to 10 μm, which is independent of the crystallographic orientations. Once the critical penetration depth is reached, the persistent islands of grain boundary (PIGB) between the break-through points would be sheared apart and the crack would "burst" into the next grain, followed by the plastic bending and final separation of ligaments that leads to the formation of radiation river markings. Thus, the fracture resistance of a grain boundary is higher than that of the single crystal, and, therefore, in a brittle material the fracture toughness is actually governed by the grain boundaries at the cleavage crack front (Qiao, 2003; Qiao and Kong, 2004). Based on the experimental results, a first-order model was developed to relate the grain boundary toughness, K_{GB}, to the crystallographic misorientations (Qiao and Argon, 2003a). However, this model predicts a negligible size dependence of K_{GB}, since the grain boundary under consideration is much wider than the distance between the break-through points. If the grain boundary width is comparable or even smaller than a single break-through point, the crack front transmission process would be constrained and consequently K_{GB} can be a function of the characteristic microstructure length. In this article, a crack trapping model is developed to analyze the grain boundary toughness in a free-standing thin film. The influences of important parameters such as film thickness, twist misorientation, and tilt misorientation are discussed in considerable detail.

2. Transmission of a cleavage front across a through-thickness grain boundary

Fig. 2 shows a high-angle grain boundary exposed in a fracture surface of a Fe–3 wt.%Si alloy. The crack flanks are separated through two mechanisms: (a) cleavage cracking of crystallographic planes and (b) plastic shear combined with shear fracture of PIGB. Compared with the former, the latter leads to a higher fracture work and requires a larger crack tip opening displacement (McClintock, 1997). As depicted in Fig. 3, as the central part of the crack front transmits from the cleavage plane of grain "A" to that of grain "B", the rest of the front is arrested by the grain boundary, being left

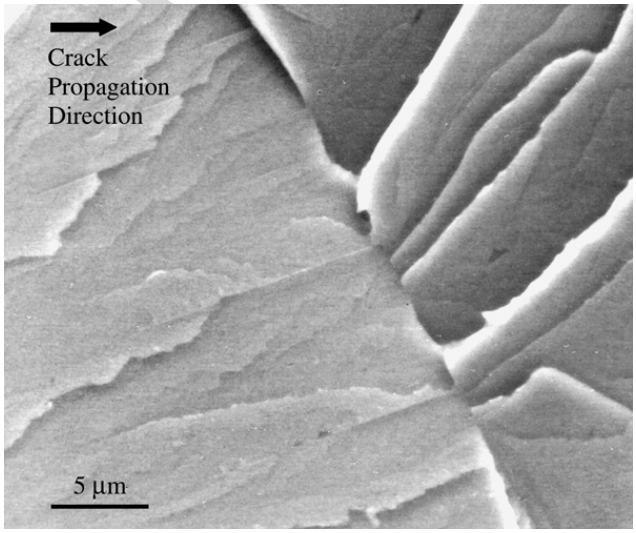

Fig. 2. SEM microscopy of cleavage cracking across a high-angle grain boundary in a Fe–3 wt.%Si alloy at −20 °C.

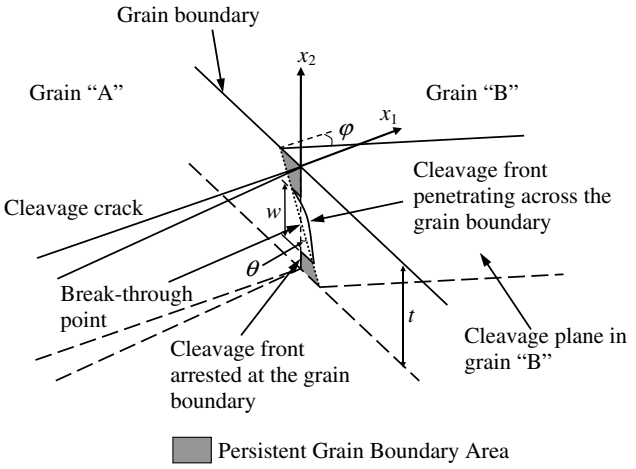

Fig. 3. A schematic diagram of the cleavage front transmission across a through-thickness grain boundary.

behind the verge of propagating. The grain boundary areas associated with the arrested crack front, which are shown as the gray areas in Fig. 3, act as bridging reinforcements, causing local crack closure. As the effective stress intensity at the crack tip increases to the critical value of K_{GB}, the crack would "jump" forward, as was observed in the experiments of iron–silicon alloys (Qiao and Argon, 2003a,b). If the cracking procedure is displacement controlled, with the constant crack opening distance, δ, the "driving force" of crack growth keeps decreasing as the crack length increases, and eventually the crack would stop in grain "B". According to a theoretical analysis (Kong and Qiao, 2005), the crack tip opening distance at the onset of the unstable crack advance across the boundary is smaller than the required value to shear apart the persistent islands of grain boundary; that is, the PIGB fail after grain "B" is cleaved. Under this condition, the persistent grain boundary areas can be regarded as impenetrable "fillers" that first hinder the crack growth by trapping effect and then bridge across the crack flanks, resulting in additional fracture resistance.

The total fracture resistance of a polycrystalline material can be decomposed as

$$G_{tot} = G_{GB} + G_b \tag{1}$$

where G_{GB} is the fracture work associated with the crack trapping effect of grain boundary, and G_b is the work of grain boundary separation. In order to calculate G_{GB}, we analyze the double-cantilever-beam (DCB) thin film sample depicted in Fig. 4. Initially, the crack tip rests at the through-thickness grain boundary between grains "A" and "B". As the crack opening distance increases quasi-statically, the cleavage front would transmit across the grain boundary (see Fig. 3). When the energy release rate

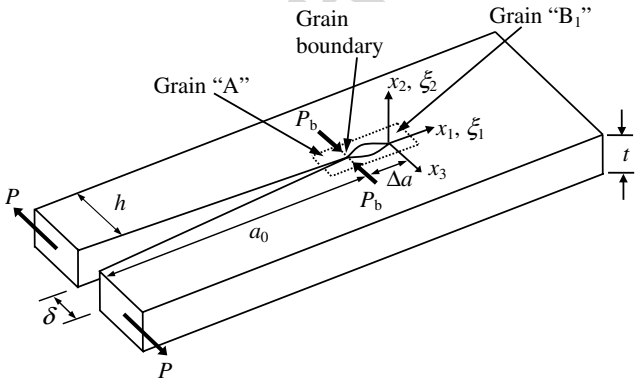

Fig. 4. The fracture of a free-standing double-cantilever-beam thin film sample.

reaches G_{GB}, the trapping effect of the PIGB is overcome. The cleavage front would bypass the grain boundary and propagate forward into grain "B", somewhat similar with a dislocation line bypassing a precipitate particle. Because, as will become clear shortly, G_{GB} is higher than the fracture resistance of grain "B", G_B, the crack front would keep advancing, until the crack growth "driving force" decreases to the critical value of crack stoppage, G_B^*. For quasi-static crack growth, G_B^* is the same as G_B. Note that $G_B = G_{sc}/(\cos\theta \cdot \cos\varphi)$, where G_{sc} is the effective surface free energy of cleavage plane, and θ and φ are the twist and the tilt misorientations across the grain boundary, respectively. During this process, the crack opening distance, δ, can be assumed to be constant.

According to the basic beam theory, we have

$$G_{GB} = \frac{3}{16}\frac{Eh^3\delta^2}{a_0^4} \tag{2}$$

where E is the modulus of elasticity, h is the height of the DCB arm, and a_0 is the initial crack length. The decrease in strain energy associated with the crack propagation is

$$\Delta U = U_0 - U_1 \tag{3}$$

where U_0 and U_1 are the strain energies before and after the crack growth, respectively. In a DCB sample, U_0 can be calculated as

$$U_0 = \frac{a_0 t}{3} G_{GB} \tag{4}$$

where t is the sample thickness.

The strain energy after the crack propagation, on the other hand, consists of two parts

$$U_1 = U_{10} + U_b \tag{5}$$

where

$$U_{10} = \frac{a_1 t}{3} G_B \tag{6}$$

is the strain energy if the grain boundary were fully separated, with a_1 being the crack length after the crack growth, and U_b is the energy caused by the bridging force, P_b, distributed in the persistence grain boundary areas, that is

$$U_b = \frac{1}{2}\int_\Omega P_b(x_2)\cdot[\tilde{\delta}(-\Delta a) - \hat{\delta}(x_2)]\,dx_2 \tag{7}$$

where Δa is the crack growth distance, $\Omega = [-t, -(t+w)/2] \cup [-(t-w)/2, 0]$,

$$\tilde{\delta}(x_1) = 2K_0 \cdot \frac{1-\nu}{\mu}\sqrt{\frac{-x_1}{2\pi}}$$

is the crack opening displacement if the grain boundary were fully separated (Ulfyand, 1965), $\hat{\delta}(x_2)$ is the shear displacement of the persistence grain boundary, v is the Poisson's ratio, μ is the shear modulus, w is the width of break-through point, and x_1 and x_2 denote the crack growth direction and the out-of-plane direction, respectively. If the bridging stress were zero, the stress intensity factor would be

$$K_0 = \sqrt{3E^2h^3\delta^2/[16a_1^4(1-v^2)]}.$$

The coordinate system of the cleavage front after the crack propagation is shown in Fig. 5. Note that $P_b(x_2) = \mu \cdot [\hat{\delta}(x_2)^2/\delta_{GB}]$, with δ_{GB} being the grain boundary thickness.

In general case, the crack advance after the crack trapping effect is overcome would be unstable, and therefore G_B^* differs from the quasi-static critical energy release rate. However, if there existed a fracture resistance gradient in grain "B" such that the local fracture resistance is always equal to the crack growth "driving force", the crack propagation is in equilibrium and the front would stop as the energy release rate decreases to G_B. Although it is clear that, under this condition, the crack growth distance is different from that of the actual case where the fracture resistance of grain "B" is a material constant, since the crack behavior subsequent to the break-through of grain boundary does not affect the critical condition, introducing in the virtual fracture resistance gradient would not affect the result of G_{GB}, as long as the excess fracture work is taken into consideration.

When the crack front is d_1 away from the grain boundary, the effective stress intensity factor at the crack tip can be calculated as (Ulfyand, 1965)

$$K(d_1, x_2) = K^* + \int_\Omega H(s, d_1, \xi_2) P_b(\xi_2)\, d\xi_2 \tag{8}$$

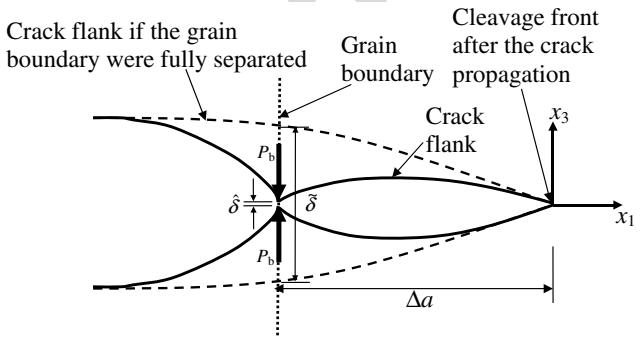

Fig. 5. The cleavage front after the crack propagation. The persistent grain boundary areas bridge across the crack flanks.

where

$$K^* = \sqrt{3E^2h^3\delta^2/[16(a_0+d_1)^4(1-v^2)]}$$

is the stress intensity factor if the persistent grain boundary did not exist;

$H(s, d_1, \xi_2) = \sqrt{2/\pi^3} \cdot \sqrt{d_1}/(s^2 + d_1^2)$,

(ξ_1, ξ_2) is the local coordinate system, as shown in Fig. 4; and $s = |x_2 - \xi_2|$. The local fracture resistance that keeps the crack growth quasi-static can then be stated as

$$\widetilde{G}(d_1) = \left(\frac{1-v^2}{tE}\right)\left\{\int_{-t}^{0}\left[K_0 + \int_\Omega H(s, d_1, \xi_2) P_b(\xi_2)\, d\xi_2\right] dx_2\right\}^2 \tag{9}$$

As the crack stops,

$$G_B = \widetilde{G}(\Delta a) \tag{10}$$

Substituting Eqs. (2), (8) and (9) into (10) gives

$$G_B = \left(\frac{1-v^2}{tE}\right)\left\{\int_{-t}^{0}\left[\sqrt{\frac{EG_{GB}}{1-v^2}}\left(\frac{a_0}{a_0+\Delta a}\right)^2 + \int_\Omega H(s, \Delta a, \xi_2) P_b(\xi_2)\, d\xi_2\right] dx_2\right\}^2 \tag{11}$$

According to the conservation of energy,

$$\frac{\Delta U}{t} = \int_0^{\Delta a} \widetilde{G}(d_1) dd_1 \tag{12}$$

Substitution of Eqs. (3)–(7) and (9) into (12) leads to

$$\begin{aligned}&\frac{1}{3}(a_0 G_{GB} - a_1 G_B) - \frac{1}{2t}\int_\Omega P_b(x_2) \cdot \left[\frac{2(1-v)}{\mu}\sqrt{\frac{EG_{GB}}{1-v^2}\frac{\Delta a}{2\pi}}\left(\frac{a_0}{a_1}\right)^2 - \sqrt{\frac{P_b(x_2)\delta_{GB}}{\mu}}\right] dx_2 \\ &= \int_0^{\Delta a}\left(\frac{1-v^2}{tE}\right)\left\{\int_{-t}^{0}\left[\sqrt{\frac{EG_{GB}}{1-v^2}}\left(\frac{a_0}{a_0+d_1}\right)^2 + \int_\Omega H(s, d_1, \xi_2) P_b(\xi_2) d\xi_2\right] dx_2\right\}^2 dd_1\end{aligned} \tag{13}$$

Finally, by taking into consideration the crack closure effect of the bridging force, we have

$$\begin{aligned}&\frac{\sqrt{P_b(x_2)\cdot\mu\cdot\delta_{GB}}}{2(1-v)} - \sqrt{\frac{EG_{GB}}{1-v^2}\frac{\Delta a}{2\pi}}\left(\frac{a_0}{a_1}\right)^2 \\ &= \int_\Omega \widehat{K}(x_2, \xi_2) P_b(\xi_2) d\xi_2\end{aligned} \tag{14}$$

where $\widehat{K}(x_2, \xi_2) = \frac{1}{|x_2-\xi_2|\pi^2} \cdot \arctan\left\{\frac{2\cdot\Delta a}{|x_2-\xi_2|}\right\}$ (Qiao et al., 2004). The procedure of calculation of G_{GB}

is now complete. Eq. (14) is a Fredholm integral equation of $P_b(x_2)$, which can be transformed into a set of algebra equations using the Ritz method. By solving Eqs. (11), (13), and (14) numerically, G_{GB} and Δa can be obtained as functions of t. Since, as previously discussed, the calculated Δa does not reflect the actual crack growth distance, in the following section we will focus on the discussion of G_{GB}.

3. Results and discussion

Eqs. (11), (13) and (14) form a nonlinear equation set that can be solved through an iteration procedure. Based on a first-order approximation of the grain boundary resistance (Qiao and Argon, 2003a), the initial value of G_{GB} was taken as $G_B\left(\frac{\sin\theta+\cos\theta}{\cos^2\varphi}+0.25\frac{\sin\theta\cos\theta}{\cos\varphi}\right)$. The initial value of Δa was set to $(G_{GB}/G_B)^{1/4}-1$, which is the crack growth length if the fracture resistance gradient, $\widetilde{G}(x_1)$, is ignored (Qiao and Kong, 2004). The bridging force was assumed to be a third order polynomial. Initially, the constant term was taken as the effective shear strength of grain boundary, τ_y, and the coefficients of higher order terms were set to zero. The numerical integration over the persistent grain boundary areas was dealt with by a coordinate transformation method, following the discussion of Pan and Amadei (1996).

Fig. 6 shows the numerical results of G_{GB}/G_B, where $v=0.3$, $E/\mu=\sqrt{3}$, and a_0/w and δ_{GB}/w are somewhat arbitrarily chosen as 200 and 0.05, respectively. Actually, the result of G_{GB} is quite insensitive to the values of v, a_0, and δ_{GB}. With a constant t/w ratio, as v varies from 0.01 to 0.49, the variation in G_{GB} is less than 5%. Since

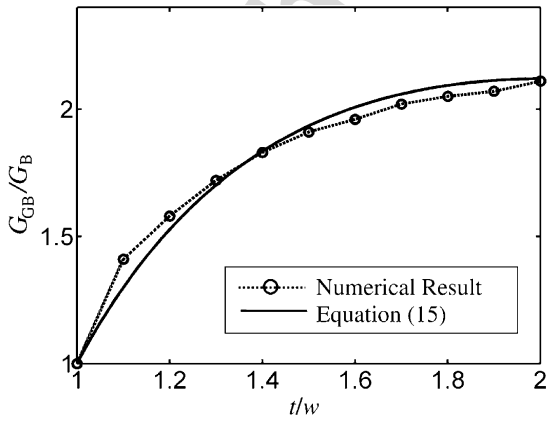

Fig. 6. The relationship between G_{GB} and t/w.

$E/\mu=\sqrt{3}$ is quite acceptable for most of the materials, it can be stated that the elastic properties have little influence on the fracture toughness of grain boundary. As a_0/w changes from 200 to 20,000, the value of G_{GB} decreases only slightly by about 3%. The weak elastic property and crack length dependences of G_{GB} are probably caused by the use of the basic beam theory in Eqs. (2) and (6), where E and a_0 come in by affecting the strain energy. When a_0 is relatively small, especially when it is comparable with the film thickness, the error of basic beam theory cannot be ignored and this model breaks down. As δ_{GB}/w varies in the range of 0.01–0.5, the variation in G_{GB} is only around 5%. As discussed in the introductory section, according to the experimental data, the width of the break-through window, w, is independent of the crystallographic orientations. Therefore, the vital factor that governs the crack trapping effect of grain boundary is the film thickness, t.

Based on a liner average analysis, Rose (1987) has obtained the analytical solution for the fracture resistance of penetrable obstacles, $w'/t'+f^2(w'/t')\cdot(1-w'/t')$, where w' is the obstacle size, t' is the spacing between obstacles, and f is a function to be determined. In this framework (Xu et al., 1998), through the mean square regression, the numerical results of G_{GB} can be expressed as

$$\frac{G_{GB}}{G_B}=\frac{w}{t}+\left(2.4-0.3\frac{t}{w}\right)^2\cdot\left(1-\frac{w}{t}\right) \tag{15}$$

When $t/w\leqslant 1$, that is, the crack front penetrate through the whole grain boundary uniformly, $G_{GB}/G_B=1$, as it should. As film thickness exceeds w, only the central part of the grain boundary can be penetrated through by the cleavage front and, thus, the value of t/w rises. Due to the crack trapping effect of the persistent grain boundary areas, G_{GB}/G_B increases rapidly to 1.8 as t/w reaches 1.5. As t/w continues to increase, the sensitivity of grain boundary toughness to the film thickness keeps decreasing, and when $t/w>1.8$, the influence of t/w on G_{GB} is only secondary. If the film thickness is much larger than the width of break-through window, there can be more than one break-through points along the crack front. Under this condition, the film thickness effect would vanish and the grain boundary toughness converges to the coarse-grain solution (Kong and Qiao, 2005). For iron–silicon alloy, w is around 2–3 μm (Qiao and Argon, 2003a). Thus, when the film thickness is in the range of 1–5 μm, the size effect of grain boundary

toughness must be taken into consideration. If the film thickness is smaller than this range, the regular break-through mode dominates the crack front transmission; and if the film thickness is above this range, the crack front behavior is governed by multiple break-through points, both of which would result in a negligible film thickness dependence of G_{GB}. Note that the values of w for different materials can be quite different, which in turn affects the transition range of film thickness.

A "by-product" of the calculation of G_{GB} is the determination of the distributed bridging force, $P_b(x_2)$, in the persistent grain boundary area, as shown in Fig. 7. As the film thickness rises, the crack trapping effect is increasingly pronounced, while the PIGB width also increases. The numerical data show that the latter effect is dominant and thereby the bridging force decreases with the film thickness. When t/w is small, the distribution of $P_b(x_2)$ is relatively uniform. The degree of uniformity is reduced as t/w ratio becomes larger. The bridging force reaches the maximum value at the border of the break-through window, and the minimum point is at the film surface. It can be seen that the maximum P_b/μ is at the level of 10^{-3}, which is in elastic domain for most of materials, indicating that the above discussion is self-compatible.

After the crack trapping effect of a grain boundary is overcome, with the increasing of remote loading, the crack would advance forward and eventually the persistent grain boundary areas would be sheared apart. The specific work of separation can be stated as

$$G_b = \frac{\gamma_{gb}\cdot\tan\theta}{2}\frac{t}{d}\left[1-\left(\frac{w}{t}\right)^2\right] \tag{16}$$

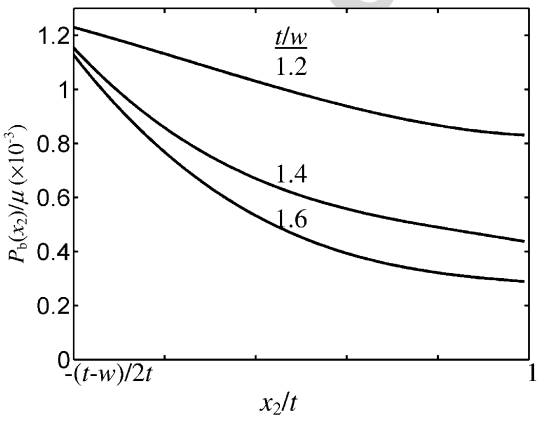

Fig. 7. The distribution of the bridging force in the persistent grain boundary area.

where d is the cross-sectional diameter of the through-thickness grain and γ_{gb} is the effective surface free energy of grain boundary. Substituting Eqs. (15) and (16) into (1) gives the overall fracture resistance of grain boundary

$$\frac{G_{tot}}{G_{sc}} = \left\{\frac{w}{t}+\left[2.4-0.3\frac{t}{w}\right]^2\cdot\left(1-\frac{w}{t}\right)\right\}\frac{1}{\cos\theta\cdot\cos\varphi} + \beta\frac{\tan\theta}{4}\frac{t}{w}\left[1-\left(\frac{w}{t}\right)^2\right] \tag{17}$$

where $\beta=\beta_1\beta_2$, $\beta_1=w/d$, and $\beta_2=(2\gamma_{gb})/G_{sc}$. For most of materials, β_2 is in the range of 0.7–0.9 (McClintock and Argon, 1993). The cross-sectional size of the grain in a thin film is determined by a number of factors such as substrate temperature, back pressure, film thickness, and heat treatment history. If the substrate temperature is low, the grain structure can be columnar and d is around 0.1–1 μm. If the substrate temperature is high, the

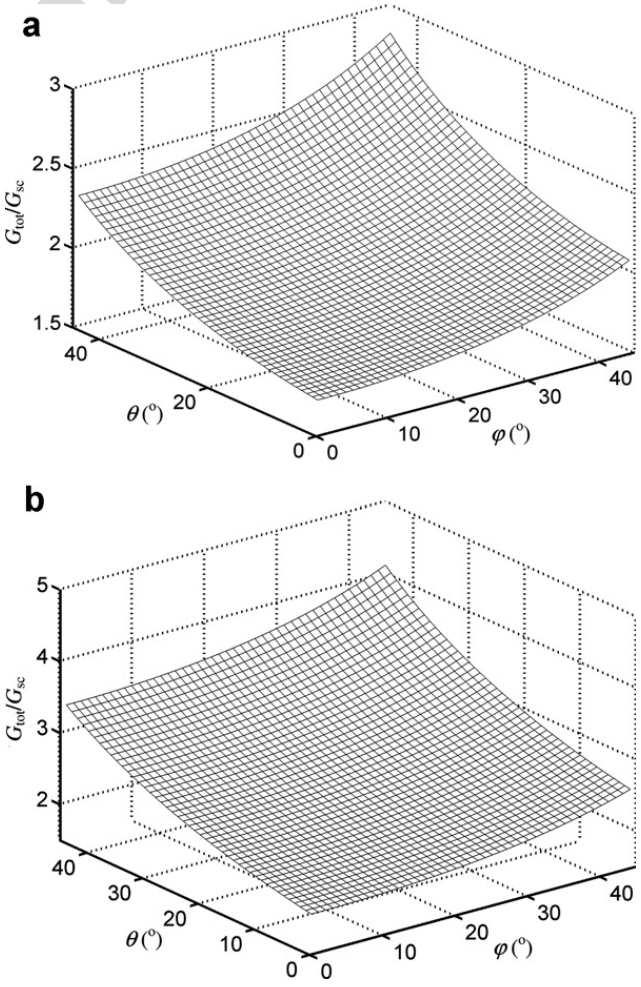

Fig. 8. The fracture resistance of a polycrystalline thin film: (a) $t/w=1.3$, and (b) $t/w=1.6$. The value of β is set to 1.5.

grain structure is equiaxed and d can be as large as 5–10 μm. Hence, for different thin film materials, the value of β_1 can range from 0.1–10. Fig. 8 shows that, similar with G_{GB}, G_{tot} increases with t/w, as it should, since both terms in Eq. (17) increases as t/w rises. The value of G_{tot} increases with both twist and tilt misorientations, and the influence of the twist angle is more important, which is in consistent with the experimental data (Gell and Smith, 1967; Qiao and Argon, 2003a,b). It can be seen that the grain boundary toughness is highly dependent on the crystallographic orientations. Depending on the film thickness, in an "average" case where $\theta = \varphi = 22.5°$, a grain boundary would lead to a 2–4 fold rise in fracture resistance, among which, as $\beta = 1$, about 70% is due to the crack trapping effect. As β increases, the work of separation of grain boundary becomes more significant.

4. Conclusions

A theoretical analysis is performed on the transmission of a cleavage crack across a through-thickness grain boundary in a free-standing thin film material. In this model, the cleavage front first penetrates across the grain boundary around a breakthrough point. The persistent grain boundary areas fail after the crack trapping effect is overcome. This analysis gives the upper bound of the grain boundary toughness. The numerical results indicate that, when the film thickness is too small or too large, the grain boundary toughness is size independent. As the film thickness is in the intermediate range, the film thickness effect must be taken into consideration. The following conclusions are drawn:

(1) There is a transition range of film thickness around 1–1.8 times of the width of breakthrough window in which the size effect is pronounced.
(2) In the transition range, as the film thickness increases the grain boundary toughness becomes larger.
(3) Below the transition range, the cleavage front transition is uniform; above the transition range, the crack trapping effect of persistent grain boundary areas is saturated.
(4) The grain boundary toughness is highly dependent on the crystallographic misorientations. The influence of the twist misorientation is more important.

Acknowledgements

This study was supported by The Office of Basic Energy Sciences, DOE under Grant No. DE-FG02-05ER46195, for which we are grateful to Dr. Yok Chen. Special thanks are also due to Professor Ali S. Argon for the help with understanding experimental observations and to Professor Ernian Pan for the help with developing computer programs.

References

Gao, H., Huang, Y., Nix, W.D., Hutchinson, J.W., 1999. Mechanism-based strain gradient plasticity – I. Theory. J. Mech. Phys. Solids 47, 1239–1263.
Gell, M., Smith, E., 1967. The propagation of cracks through grain boundaries in polycrystalline 3% silicon iron. Acta Metall. 15, 253–258.
Hutchinson, J.W., Evans, A.G., 2000. Mechanics of materials: top-down approaches to fracture. Acta Mater. 48, 125–135.
Kong, X., Qiao, Y., 2005. Crack trapping effect of persistent grain boundary islands. Fatigue Fract. Eng. Mater. Struct. 28, 753–758.
Madou, M.J., 2002. Fundamentals of Microfabrication. CRC Press, NY, pp.123–183.
McClintock, M.A., 1997. A three dimensional model for polycrystalline cleavage and problems in cleavage after extended plastic flow or cracking. In: Chong, K. (Ed.), George R. Irwin Symposium. TMS, Warendale, PA, p. 81.
McClintock, M.A., Argon, A.S., 1993. Mechanical Behaviors of Materials. CBLS, Marietta, Ohio.
Ohring, M., 2002. The Materials Science of Thin Films. Academic Press, San Diego, CA.
Pan, E., Amadei, B., 1996. Fracture mechanics analysis of cracked 2D anisotropic media with a new formulation of the boundary element method. Int. J. Fract. 77, 161–174.
Qiao, Y., 2003. Modeling of resistance curve of high-angle grain boundary in Fe–3wt%Si alloy. Mater. Sci. Eng. A361, 30–357.
Qiao, Y., Argon, A.S., 2003a. Cleavage cracking resistance of high angle grain boundaries in Fe–3wt.%Si alloy. Mech. Mater. 35, 313–331.
Qiao, Y., Argon, A.S., 2003b. Cleavage crack-growth-resistance of grain boundaries in polycrystalline Fe–2 wt.%Si alloy: experiments and modeling. Mech. Mater. 35, 129–154.
Qiao, Y., Kong, X., 2004. An energy analysis of the grain boundary behavior in cleavage cracking in Fe–3 wt.% alloy. Mater. Lett. 58, 3156–3160.
Qiao, Y., Kong, X., Pan, E., 2004. Fracture toughness of thermoset composites reinforced by perfectly bonded impenetrable short fibers. Eng. Fract. Mech. 71, 2621–2633.
Rose, L.R.F., 1987. Toughening due to crack-front interaction with a second-phase dispersion. Mech. Mater. 6, 11–15.
Ulfyand, Y.S., 1965. Survey of Articles on the Application of Integral Transforms in Theory of Elasticity. University of North Carolina, Raleigh, NC.
Xu, G., Bower, A.F., Ortiz, M., 1998. The influence of crack trapping on the toughness of fiber reinforced composites. J. Mech. Phys. Solids 46, 1815–1833.